Kondo effect in normal-superconductor quantum dots

J. C. Cuevas,[1,2] A. Levy Yeyati,[1] and A. Martín-Rodero[1]
[1]*Departamento de Física Teórica de la Materia Condensada C-V, Universidad Autónoma de Madrid, E-28049 Madrid, Spain*
[2]*Institut für Theoretische Festkörperphysik, Universität Karlsruhe, 76128 Karlsruhe, Germany*
(Received 6 November 2000; published 12 February 2001)

We study the transport properties of a quantum dot coupled to a normal and a superconducting lead. The dot is represented by a generalized Anderson model. Correlation effects are taken into account by an appropriate self-energy that interpolates between the limits of weak and strong coupling to the leads. The transport properties of the system are controlled by the interplay between the Kondo effect and Andreev reflection processes. We show that, depending on the parameters' range, the conductance can either be enhanced or suppressed as compared to the normal case. In particular, by adequately tuning the coupling to the leads one can reach the maximum value $4e^2/h$ for the conductance.

DOI: 10.1103/PhysRevB.63.094515 PACS number(s): 74.50.+r, 72.15.Qm, 73.23.Hk

The Kondo effect is a prototypical correlation effect in solid state physics. Although it was first analyzed for the case of magnetic impurities in metals, in the last years there has been a renewed interest in Kondo physics with its observation in a semiconductor quantum dot (QD).[1,2] Quantum dots constitute an ideal laboratory for testing the theoretical predictions as they allow to vary the relevant parameters in the problem in a controlled way. This technology also opens some new possibilities like the exploration of the Kondo effect when the dot is connected to superconducting leads. The interesting issue in this case is related to the competition between the strong Coulomb interaction in the quantum dot and the pairing interaction within the leads.

From the theoretical side, the Kondo effect in QD's has been mainly analyzed by means of the single-level Anderson model.[3,4] The theory predicts an enhancement of the dot conductance at low temperatures due to the development of the so-called Kondo resonance. The case when one of the leads is superconducting has been recently analyzed by some authors using different theoretical methods[5–7] assuming a modified Anderson model in which one of the metallic electrodes is substituted by a BCS superconductor. While some authors have predicted an enhancement of the conductance due to Andreev reflection at the superconducting lead,[6] others have predicted the opposite effect.[7] In Refs. 5 and 7 the infinite charging energy limit ($U\rightarrow\infty$) has been assumed. However, in an actual experiment, this assumption may not be completely justified (for instance, in the experiments of Ref. 1 the ratio U/Γ, Γ being the dot tunneling rate, was estimated to be around 6.5). The approach presented in this paper would allow to analyze this problem for a broad range of the different parameters of the model. We will show that, depending on the values of these parameters, one can obtain either an enhancement or a reduction of the conductance with respect to the normal case.

Our approximation scheme is based on the hypothesis that a good approximation to the electron self-energy can be found by interpolating between the limits of weak and strong coupling to the leads. This interpolative method has been applied successfully to analyze different strongly correlated electron systems like the equilibrium,[8,9] the nonequilibrium,[4] and the multilevel[10] Anderson models and the Hubbard model.[11,12] In this paper we shall discuss how to extend this method to the superconducting case.

For describing a N-QD-S system we use an Anderson-like Hamiltonian

$$\hat{H}=\hat{H}_N+\hat{H}_S+\sum_\sigma \epsilon_0\hat{n}_\sigma+U\hat{n}_\uparrow\hat{n}_\downarrow+\hat{H}_T, \qquad (1)$$

where $\hat{n}_\sigma=\hat{d}_\sigma^\dagger\hat{d}_\sigma$, $\hat{H}_N$ and $\hat{H}_S$ represent the uncoupled normal and superconducting leads respectively; $\hat{H}_T=\Sigma_{k\in N,S;\sigma}t_{0,k}\hat{d}_\sigma^\dagger\hat{c}_{k,\sigma}+\text{H.c.}$ describing the coupling between the dot level and the leads. Within this model the dot is represented by a single-spin degenerate level with a repulsive Coulomb interaction described by the U-term in Eq. (1). We shall assume that the superconducting lead is well described by the BCS theory with a superconducting gap Δ and the normal lead is, as usual, characterized by a flat density of states around the Fermi level, ρ_F.

The transport properties of this model can be obtained by means of Green-function techniques. In order to analyze the linear regime the main quantity to be determined is the dot retarded Green function, which in a Nambu 2×2 representation adopts the form

$$\hat{G}^r(\omega)=[\omega\hat{I}-\epsilon_0\hat{\sigma}_z-\hat{\Sigma}^r(\omega)-\hat{\Gamma}_N(\omega)-\hat{\Gamma}_S(\omega)]^{-1}, \qquad (2)$$

where $\hat{\Gamma}_N$ and $\hat{\Gamma}_S$ are the tunneling rates given by $\hat{\Gamma}_N=\Gamma_L\hat{I}$, and the superconducting tunneling rate $\hat{\Gamma}_S$ is given by $\hat{\Gamma}_S=\Gamma_R\hat{g}$, where $\Gamma_{L,R}=\pi t_{L,R}^2\rho_F$, $g_{11}=g_{22}=-\omega/\sqrt{\Delta^2-\omega^2}$, and $g_{12}=g_{21}=\Delta/\sqrt{\Delta^2-\omega^2}$ (the chemical potential of the superconducting lead is taken as zero). The self-energy $\hat{\Sigma}^r(\omega)$ takes into account the effect of Coulomb interactions. To the lowest order in U this is given by the Hartree-Fock Bogoliubov approximation: $\hat{\Sigma}^r=U\langle\hat{n}\rangle\hat{\sigma}_z+\Delta_d\hat{\sigma}_x$, Δ_d being the proximity effect induced order parameter in the QD, $\Delta_d=U\langle\hat{d}_\uparrow^\dagger\hat{d}_\downarrow^\dagger\rangle$. The crucial problem is to find a good approximation to include correlation effects beyond this mean-field approximation.

Within the spirit of the interpolative method commented above, the self-energy is constructed in such a way as to

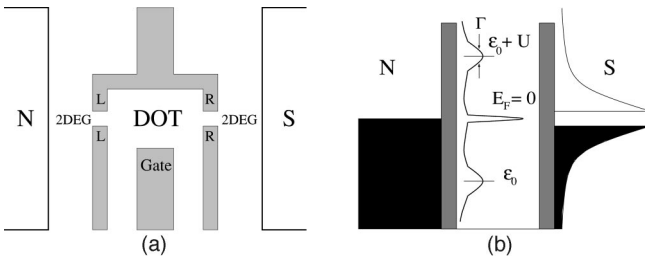

FIG. 1. (a) Schematic representation of a quantum dot coupled to a normal and a superconducting lead. (b) Schematic energy diagram of this system, showing the local density of states in the dot with the charging states at ϵ_0 and ϵ_0+U and the sharp Kondo resonance at the Fermi level.

interpolate between the limits of weak and strong coupling to the leads for which the exact result is known. Let us first analyze the weak coupling or *atomic* limit. In this case we have $t_{L,R}/U \to 0$ and thus $\hat{\Gamma}_N/U$, $\hat{\Gamma}_S/U \to 0$. In this limit the induced order parameter in the QD vanishes faster than $(t_R/U)^2$ and one can neglect the nondiagonal elements in the self-energy matrix. On the other hand, the diagonal elements can be easily evaluated in this limit using the equation of motion method[8] and have the form

$$\Sigma^r_{11,22} \to \pm U\langle\hat{n}\rangle + \frac{U^2\langle\hat{n}\rangle(1-\langle\hat{n}\rangle)}{\omega \mp \epsilon_0 \mp U(1-\langle\hat{n}\rangle)}. \tag{3}$$

In the opposite limit, $U/t_{L,R} \to 0$, one can accurately evaluate the self-energy using standard perturbation theory in the Coulomb interaction. The different diagrams contributing to the second-order self-energy are depicted in Fig. 1. In the superconducting case, there appear additional diagrams to the one in the normal case [diagram (a)] corresponding to the interaction of an electron with an electron-hole pair in the QD; the remaining diagrams contain at least one anomalous propagator and vanish identically in the normal state. As in the normal case,[4] the nonperturbed one-electron Hamiltonian, over which the diagrammatic series is constructed, is taken as an effective mean field, characterized by an effective dot level ϵ_{eff}, having the same dot charge as the fully interacting problem. As shown in Ref. 4 this self-consistency condition provides in the normal case a good fulfillment of the Friedel sum rule at zero temperature. The extension of this procedure to the superconducting case requires dressing the propagators in the diagrams of Fig. 2 with the nondiagonal self-energy Σ_{12} in order to impose also consistency in the nondiagonal charge $\langle \hat{d}^\dagger_\uparrow \hat{d}^\dagger_\downarrow \rangle$. Notice that although the interaction in the QD is repulsive, there is always some induced paring potential in the dot due to the proximity effect. The inclusion of this effect for finite U turns out to be crucial for the correct description of the dot electronic and transport properties.

The original interpolative scheme stems from the observation that the second-order self-energy ($\Sigma^{(2)}$) has a similar functional form as the atomic self-energy for large frequencies[8] thus allowing for a smooth interpolation between the two limits. In the superconducting case, the diagonal elements of the second order self-energy behave as

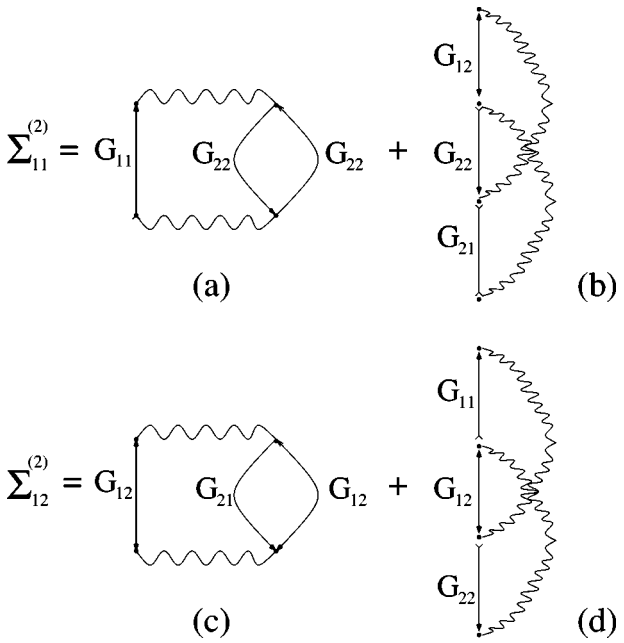

FIG. 2. Second-order self-energy diagrams.

$$\Sigma^{(2)}_{11,22} \sim \frac{U^2\langle\hat{n}\rangle(1-\langle\hat{n}\rangle)}{\omega \mp \epsilon_{eff}} \tag{4}$$

for large frequencies, while the nondiagonal elements decay faster than U^2/ω. This behavior permits to define a Nambu 2×2 interpolative ansatz for the self-energy matrix as

$$\hat{\Sigma}(\omega) = U\langle\hat{n}\rangle\hat{\sigma}_z + \Delta_d\hat{\sigma}_x + [\hat{I} - \alpha\hat{\Sigma}^{(2)}\hat{\sigma}_z]^{-1}\hat{\Sigma}^{(2)}(\omega), \tag{5}$$

where

$$\alpha = \frac{\epsilon_0 + (1-\langle\hat{n}\rangle)U - \epsilon_{eff}}{U^2\langle\hat{n}\rangle(1-\langle\hat{n}\rangle)},$$

and $\hat{\Sigma}^{(2)}$ is the second order self-energy matrix whose elements are given by the diagrams depicted in Fig. 2.

Using this ansatz one recovers the correct behavior of the self-energy both in the weak and strong coupling limits. Moreover, this ansatz satisfies the exact relations between the different matrix elements, i.e., $\Sigma_{12}(\omega) = \Sigma_{21}(\omega)$ and $\Sigma_{11}(\omega) = -\Sigma^*_{22}(-\omega)$.

In order to test the accuracy of our approximation we first study a simple toy model, not intended to represent a realistic situation but which can be solved exactly. This is a two-sites model, described by the following Hamiltonian:

$$\hat{H} = \sum_\sigma \epsilon_0\hat{n}_\sigma + t(\hat{d}^\dagger_\sigma\hat{c}_\sigma + \text{H.c.}) + U\hat{n}_\uparrow\hat{n}_\downarrow + (\Delta\hat{c}_\downarrow\hat{c}_\uparrow + \text{H.c.}), \tag{6}$$

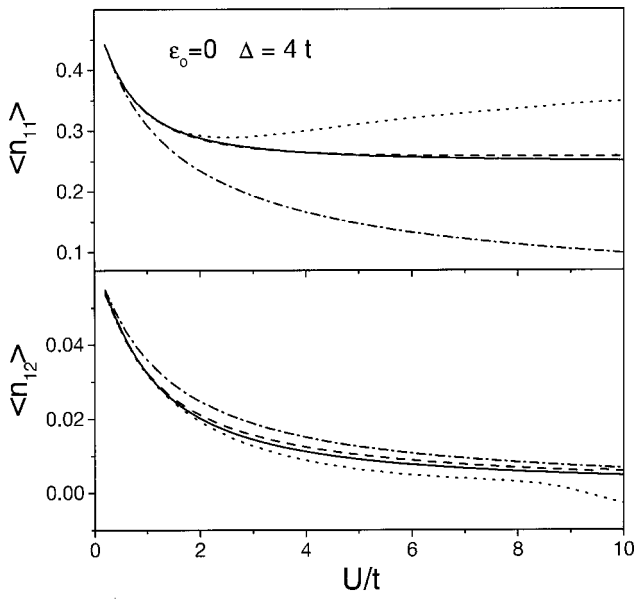

FIG. 3. Diagonal and nondiagonal charge for the toy-model two-level system discussed in the text as a function of U/t: exact solution (full line), interpolated self-energy (dashed), second-order self-energy (dotted) and first-order approximation (dashed-dotted).

where we replace the superconducting electrode by a single site with a paring potential Δ. The exact ground state is obtained combining all possible configurations with a different number of electrons.

Figure 3 shows the behavior of the charge and the induced order parameter at the dot site as a function of U for $\epsilon_0=0$, $\Delta=0.1$, and $t=0.4$. As can be observed, the interpolative approach improves substantially the results given by the first order (Hartree-Fock Bogoliubov) and the second-order calculations, following closely the exact result. It is remarkable how the interpolative self-energy eliminates some pathologies of the second-order approximation like the increase of the dot charge for intermediates values of U. This good agreement with the exact results is also found regardless of the position of the dot level and the ratio t/Δ. Only for the limit $t \ll \Delta$ one finds a somewhat larger discrepancy in the dot charge. We should point out that, although this model is only introduced as a test of the approximation, it provides nevertheless a rough description of the behavior of the charge and the induced pairing potential in a model with a continuous density of states for the superconducting electrode.

Let us analyze now the continuous model given by Eq. (1). Due to the presence of an additional energy scale fixed by Δ, the number of different physical regimes is larger than in the normal case. We will mainly consider the more interesting physical regime $\Gamma=\Gamma_L+\Gamma_R\sim\Delta$.[13] In Fig. 4(a) we show the dot spectral density (LDOS) for a symmetric case ($\epsilon_0=-U/2$) with $\Gamma_L=\Gamma_R=\Delta$ and increasing values of U. As can be observed, when $U\leqslant\Delta$ the LDOS exhibits a double peak around the Fermi energy that is due to the influence of the superconducting electrode by the proximity effect. However, as U increases, the double peak is replaced by a single narrow Kondo resonance as in the normal case. The comparison with the normal case reveals that the Kondo resonance gets narrower in the superconducting case and its height increases with U above the normal value. In the limit $U\to\infty$, this height approaches the value $2/(\pi\Gamma)$, which is twice the value in the normal case at zero temperature, as fixed by the Friedel sum rule. The narrowing of the Kondo resonance gives rise to a lowering of the Kondo temperature with respect to the normal case.

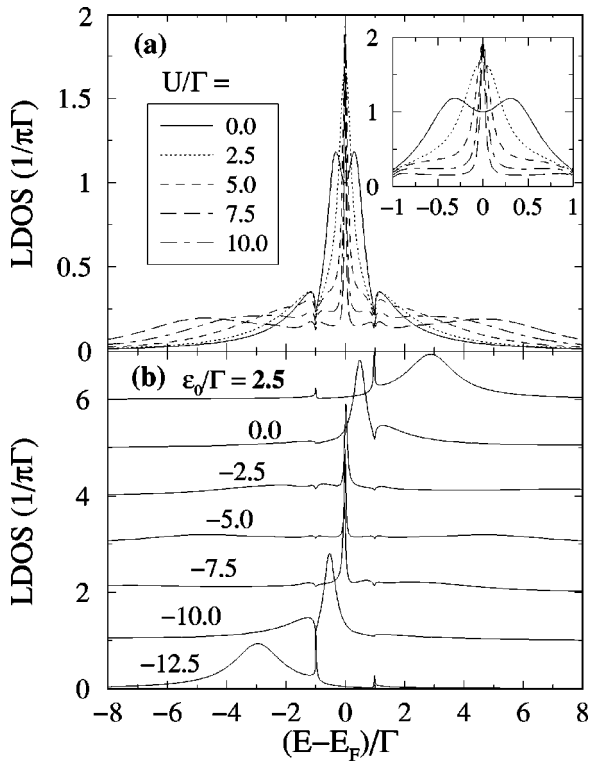

FIG. 4. (a) Dot spectral density in the symmetric case ($\epsilon_0=-U/2$ and $\Gamma_L=\Gamma_R$) with $\Gamma=\Delta$ for different values of U/Γ. The inset shows a blowup of the region around the Fermi energy. (b) Dot spectral density for different values of ϵ_0 with $U=10\Gamma$ and $\Gamma=\Delta$.

For energies larger than Δ the differences between the normal and the superconducting LDOS become negligible, with the usual broad resonances at ϵ_0 and ϵ_0+U that become more pronounced for increasing U.

By varying the dot level position ϵ_0 one can study the transition from the Kondo to the mixed valence regime. The evolution of the dot LDOS is illustrated in Fig. 4(b). When approaching the mixed valence regime ($|\epsilon_0|<\Gamma$ or $|\epsilon_0+U|<\Gamma$) the Kondo resonance is replaced by an asymmetric broad resonance close to the Fermi energy as in the normal case. In the superconducting case, however, the LDOS develops an additional structure associated with the BCS divergencies at the gap edges.[7]

As in any NS contact, transport at low voltages is possible due to Andreev reflection processes. At finite temperature, the linear conductance is given by the expression[14]

$$G=\frac{16e^2}{h}\Gamma_L\int_{-\infty}^{\infty}dE\,\mathrm{Im}(G_{12}^{r}G_{11}^{a})(\Gamma_R-\mathrm{Re}\,\Sigma_{12})\left(-\frac{\partial f}{\partial E}\right), \tag{7}$$

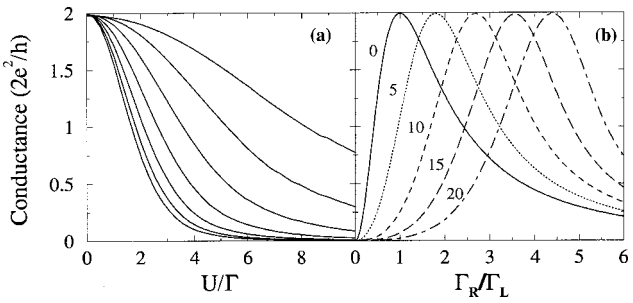

FIG. 5. (a) Conductance at zero temperature for the symmetric case as a function of U/Γ and for different values of Γ/Δ. From bottom to top $\Gamma/\Delta=$ 0.125, 0.25, 0.5, 1.0, 2.0, 4.0, and 8.0. (b) Same as (a) for asymmetric coupling to the leads as a function of Γ_R/Γ_L and different values of U/Γ_L.

where $f(E)$ is the Fermi function. At zero temperature, $\mathrm{Im}\,\hat{\Sigma}(0)=0$, and Eq. (7) reduces to

$$G=\frac{4e^2}{h}\frac{4\Gamma_L^2\tilde{\Gamma}_R^2}{[\tilde{\epsilon}^2+\Gamma_L^2+\tilde{\Gamma}_R^2]^2}, \tag{8}$$

where $\tilde{\Gamma}_R=\Gamma_R-\mathrm{Re}\,\Sigma_{12}(0)$ and $\tilde{\epsilon}=\epsilon_0+\mathrm{Re}\,\Sigma_{11}(0)$. Notice that Eq. (8) coincides at $U=0$ with the well known noninteracting result.[15]

One would expect that for a dot symmetrically coupled to the leads (i.e., $\Gamma_L=\Gamma_R$) and in the case of electron-hole symmetry ($\epsilon_0=-U/2$), the conductance should reach its maximum value $4e^2/h$[6]. However, the actual situation is more complex due to the reduction of the induced paring amplitude in the dot arising from the repulsive Coulomb interaction. As a consequence the conductance decreases for increasing U even in this case. This decrease is illustrated in Fig. 5(a) where we plot the conductance as a function of U in the symmetric case for different values of Γ/Δ. For large U/Γ we find that the conductance decreases roughly as $(\Gamma/U)^4$. This behavior can be understood as follows: in order to have a vanishing pairing amplitude in the $U/\Gamma\to\infty$ limit, the nondiagonal self-energy Σ_{12} should tend to cancel the nondiagonal tunneling rate $(\hat{\Gamma}_S)_{12}$. By analyzing the expression of diagram (d) in Fig. 2, this requires that G_{12} decays as $(\Gamma/U)^2$ and therefore the conductance given by Eq. (7) in our approximation should decay roughly as $(\Gamma/U)^4$. This decay is probably less pronounced than in the exact solution where one would rather expect an exponential behavior in the Kondo regime.

Although the previous analysis shows that the maximum value for the conductance $4e^2/h$ can never be reached in the symmetric case for finite U, this is not necessarily the case for an asymmetric situation with $\Gamma_L\neq\Gamma_R$. In fact, if the coupling to the electrodes could be tuned in order to reach the condition $\tilde{\Gamma}_R=\Gamma_L$ then Eq. (7) predicts a maximum in the value of G. As shown in Fig. 5(b), this condition can be reached by increasing the coupling to the superconducting electrode. The ratio between Γ_R and Γ_L at the maximum becomes larger for increasing U. In a situation with electron-hole symmetry, like the one depicted in Fig. 5(b), the conductance at zero temperature reaches its maximum possible value $4e^2/h$.

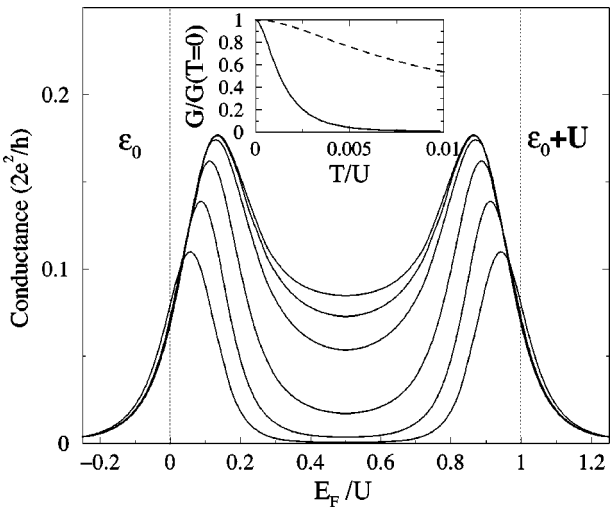

FIG. 6. Conductance for different temperature values: $U=10\Gamma$, $\Delta=\Gamma/2$ and $T/U=$ 0.0, 0.0005, 0.001, 0.0025, 0.005, 0.01. Inset: normalized conductance as a function of temperature for N-dot-S (full line) and N-dot-N (dashed line) at $E_F=U/2$.

In normal quantum dots a signature of the Kondo effect is given by an anomalous temperature dependence in the linear conductance,[1] which exhibits a continuous transition from a maximum conductance in the Kondo regime to well-resolved conductance peaks associated with Coulomb blockade. When one of the electrodes is superconducting, there is also a decrease of conductance with temperature in the Kondo regime. However, as depicted in Fig. 6, the conductance already exhibits a double-peaked structure at zero temperature when $\Gamma_L=\Gamma_R$. The reduction of conductance with temperature is in this case much faster than in the normal case, as shown in Fig. 6 (inset). This difference is a consequence of the lowering of the Kondo temperature due to the presence of the superconducting electrode.

In conclusion, we have analyzed the electronic transport properties of a quantum dot coupled to a normal and a superconducting lead. For this purpose we have introduced an electron self-energy that interpolates between the limits of weak and strong coupling to the leads, an approach that has been previously used for normal systems.[4,8–12] This approximation allows to describe a broad range of parameters including the relevant one for an actual experiment. On the other hand, we have shown that for finite charging energy the dot conductance can either be enhanced or suppressed with respect to the normal case. While in a symmetrically coupled dot ($\Gamma_L=\Gamma_R$) an increasing charging energy tends to reduce the conductance, in the asymmetric case it is always possible to reach a maximum in the conductance by fine tuning the coupling to the superconducting electrode. In the case of electron-hole symmetry this maximum reaches the value $4e^2/h$ at zero temperature. The predictions presented in this work could be tested experimentally using similar technologies to those currently used for normal quantum dots.[1,2,16]

We thank Jan von Delft, Hans Kroha, Gerd Schön, and Andrei Zaikin for fruitful discussions. This work was supported by the Spanish CICYT under Contract No. PB97-0044 and by the SFB 195 of the German Science Foundation. J.C. Cuevas acknowledges the European Community for funding under Contract HPMF-CT-1999-00165.

[1] D. Goldhaber-Gordon *et al.*, Nature (London) **391**, 156 (1998); Phys. Rev. Lett. **81**, 5225 (1998).
[2] S.M. Cronenwett *et al.*, Science **281**, 540 (1998).
[3] L.I. Glazman and M.E. Raikh, Pis'ma Zh. Éksp. Teor. **47**, 378 (1988) [J. Exp. Theor. Phys. **47**, 452 (1988); S. Hershfield, J.H. Davis, and J.W. Wilkins, Phys. Rev. Lett. **67**, 3720 (1991); Y. Meir, N.S. Wingreen, and P.A. Lee, *ibid.* **70**, 2601 (1993).
[4] A. Levy Yeyati, A. Martín-Rodero, and F. Flores, Phys. Rev. Lett. **71**, 2991 (1993).
[5] R. Fazio and R. Raimondi, Phys. Rev. Lett. **80**, 2913 (1998); **82**, 4950 (1999).
[6] K. Kang, Phys. Rev. B **58**, 9641 (1998).
[7] A.A. Clerk, V. Ambegaokar, and S. Hershfield, Phys. Rev. B **61**, 3555 (2000).
[8] A. Martín-Rodero *et al.*, Solid State Commun. **44**, 911 (1982).
[9] O. Takagi and T. Sasso, J. Phys. Soc. Jpn. **68**, 2894 (1999).
[10] A. Levy Yeyati, F. Flores, and A. Martín-Rodero, Phys. Rev. Lett. **83**, 600 (1999).
[11] A. Martín-Rodero *et al.*, Phys. Rev. B **33**, 1814 (1986).
[12] H. Kajueter and G. Kotliar, Phys. Rev. Lett. **77**, 131 (1996).
[13] Moreover, this could be the case of an actual experimental set up obtained by combining the semiconducting quantum dots used in Ref. 1, where Γ was estimated to be of the order of 0.1 meV, with superconducting leads. Notice that the energy gap in a traditional superconductor like Al would be of the same order.
[14] P. Schwab and R. Raimondi, Phys. Rev. B **59**, 1637 (1999).
[15] C.W.J. Beenakker, Phys. Rev. B **46**, 12 841 (1992).
[16] H. Takayanagi (private communication).